

ITO-free large-area organic solar cells

Seungkeun Choi, William J. Potscavage, Jr., and Bernard Kippelen*

School of Electrical and Computer Engineering and Center for Organic Photonics and Electronics, 777 Atlantic Dr.,
Atlanta, Georgia 30332, USA

*kippelen@gatech.edu

Abstract: We report on large-area pentacene / C₆₀ organic solar cells in which indium-tin-oxide (ITO) is replaced with a conductive polymer electrode and a 5 μm-thick metal grid is used to reduce resistive power losses. The performance of cells with the polymer electrode was compared with that of pentacene / C₆₀ devices using ITO as the transparent electrode. For large-area devices (7.3 cm²) on glass substrates with an integrated metal grid, the performance of a device with the polymer electrode is comparable to that of a device with an ITO electrode combined with a grid.

©2010 Optical Society of America

OCIS codes: (350.6050) Solar energy; (040.5350) Photovoltaics; (160.0160) Optoelectronics; (310.6860) Thin films, optical properties; (310.7005) Transparent conductive coatings

References and Links

1. B. Kippelen and J.-L. Bredas, "Organic photovoltaics," *Energy Environmental Science* **2**(3), 251–261 (2009).
2. US Geological Survey, "<http://minerals.usgs.gov/minerals/pubs/commodity/indium/>
3. S.-I. Na, S.-S. Kim, J. Jo, and D.-Y. Kim, "Efficient and Flexible ITO-Free Organic Solar Cells Using Highly Conductive Polymer Anodes," *Adv. Mater.* **20**(21), 4061–4067 (2008).
4. R. Paetzold, K. Heuser, D. Henseler, S. Roeger, G. Wittmann, and A. Winnacker, "Performance of flexible polymeric light-emitting diodes under bending conditions," *Appl. Phys. Lett.* **82**(19), 3342–3344 (2003).
5. W. J. Potscavage, Jr., S. Yoo, and B. Kippelen, "Origin of the open-circuit voltage in multilayer heterojunction organic solar cells," *Appl. Phys. Lett.* **93**(19), 193308 (2008).
6. Y. Zhou, F. Zhang, K. Tvingstedt, S. Barrau, F. Li, W. Tian, and O. Inganäs, "Investigation on polymer anode design for flexible polymer solar cells," *Appl. Phys. Lett.* **92**(23), 233308 (2008).
7. G. P. Kushto, W. Kim, and Z. H. Kafafi, "Flexible organic photovoltaics using conducting polymer electrodes," *Appl. Phys. Lett.* **86**(9), 093502 (2005).
8. J. Meiss, M. K. Riede, and K. Leo, "Towards efficient tin-doped indium oxide (ITO)-free inverted organic solar cells using metal cathodes," *Appl. Phys. Lett.* **94**(1), 013303 (2009).
9. B. O'Connor, C. Haughn, K.-H. An, K. P. Pipe, and M. Shtein, "Transparent and conductive electrodes based on unpatterned, thin metal films," *Appl. Phys. Lett.* **93**(22), 223304 (2008).
10. J. C. Bernède, Y. Berredjem, L. Cattin, and M. Morsli, "Improvement of organic solar cell performances using a zinc oxide anode coated by an ultrathin metallic layer," *Appl. Phys. Lett.* **92**(8), 083304 (2008).
11. J.-Y. Lee, S. T. Connor, Y. Cui, and P. Peumans, "Solution-processed metal nanowire mesh transparent electrodes," *Nano Lett.* **8**(2), 689–692 (2008).
12. K. Tvingstedt, and O. Inganäs, "Electrode Grids for ITO Free Organic Photovoltaic Devices," *Adv. Mater.* **19**(19), 2893–2897 (2007).
13. M.-G. Kang, M.-S. Kim, J. Kim, and L. J. Guo, "Organic Solar Cells Using Nanoimprinted Transparent Metal Electrodes," *Adv. Mater.* **20**, 4308–4313 (2008).
14. J. Zou, H.-L. Yip, S. K. Hau, and A. K.-Y. Jen, "Metal grid/conducting polymer hybrid transparent electrode for inverted polymer solar cells," *Appl. Phys. Lett.* **96**(20), 203301 (2010).
15. S. Choi, W. J. Potscavage, Jr., and B. Kippelen, "Area-scaling of organic solar cells," *J. Appl. Phys.* **106**(5), 054507 (2009).
16. B. Zimmermann, M. Glatthaar, M. Niggemann, M. K. Riede, A. Hinsch, and A. Gombert, "ITO-free wrap through organic solar cells—A module concept for cost-efficient reel-to-reel production," *Sol. Energy Mater. Sol. Cells* **91**(5), 374–378 (2007).
17. F. C. Krebs, "All solution roll-to-roll processed polymer solar cells free from indium-tin-oxide and vacuum coating steps," *Org. Electron.* **10**(5), 761–768 (2009).
18. S. Choi, W. J. Potscavage, Jr., and B. Kippelen, "Area-scaling of Organic Solar Cells and Integrated Modules," in *Organic Materials and Devices for Sustainable Energy Systems*, J. Xue, ed. (Mat. Res. Soc. Symp. Proc., Boston, MA, USA, 2009), p. S06.
19. S. Yoo, B. Domercq, and B. Kippelen, "Efficient thin-film organic solar cells based on pentacene/C₆₀ heterojunctions," *Appl. Phys. Lett.* **85**(22), 5427–5429 (2004).
20. S. Yoo, W. J. Potscavage, Jr., B. Domercq, S.-H. Han, T.-D. Li, S. C. Jones, R. Szoszkiewicz, D. Levi, E. Riedo, S. R. Marder, and B. Kippelen, "Analysis of improved photovoltaic properties of pentacene/C₆₀ organic solar

- cells: effects of exciton blocking layer thickness and thermal annealing," *Solid-State Electron.* **51**(10), 1367–1375 (2007).
21. F. Nüesch, L. J. Rothberg, E. W. Forsythe, Q. T. Le, and Y. Gao, "A photoelectron spectroscopy study on the indium tin oxide treatment by acids and bases," *Appl. Phys. Lett.* **74**(6), 880–882 (1999).
 22. A. R. McGhie, A. F. Garito, and A. J. Heeger, "A gradient sublimator for purification and crystal growth of organic donor and acceptor molecules," *J. Cryst. Growth* **22**(4), 295–297 (1974).
 23. Solarmer Energy, "<http://www.solarmer.com/>" (2010)
-

1. Introduction

Low cost and high flexibility are two key features that organic electronics can offer [1]. At the moment, indium-tin-oxide (ITO) is the most widely used transparent electrode for both organic photovoltaics (OPVs) and organic light-emitting diodes (OLEDs) since ITO has relatively high conductance compared to most other electrodes with high optical transmittance in the visible part of the spectrum. However, the high demand for indium in devices such as liquid-crystal panels and touch-screen displays has created strong price volatility for indium [2] and has generated supply concerns. The latter is a consequence of its mining which is associated with that of zinc, making its supply dependent on the demand for zinc. These factors are driving the development of ITO substitutes for organic photovoltaic technologies. Furthermore, ITO has poor mechanical properties when deposited on flexible substrates as it is susceptible to cracks when the substrates are bent below a critical bending radius of 8 mm, thus preventing the realization of high flexibility [3,4]. Hence, developing an OPV architecture in which ITO is replaced with a transparent, low-cost, and crack-tolerant electrode is of great interest [5].

Several approaches have been used in prior studies to find substitutes to the transparent conductive electrode ITO in OPV devices. They include the use of intrinsically conductive polymers such as poly(3,4-ethylenedioxythiophene):poly(styrenesulfonate) (PEDOT:PSS) [3,6,7], or very thin metal layers (10–20 nm) [8,9], combinations of thin metal layers with metal oxides such as Au with aluminum doped zinc oxide (Al:ZnO) [10], or polymers containing metal nanostructures such as meshes of metal nanowires [11]. To obtain sheet resistance values comparable to those of ITO (10–15 $\Omega/\text{sq.}$), PEDOT:PSS was also combined with thin metal grids (with a thickness generally less than 100 nm) using various processing techniques [12–14]. While all these strategies can achieve a performance comparable to that of ITO in terms of transmittance and sheet resistance, they generally do not provide solutions to the fabrication of large-area cells. A detailed analysis of the area scaling of organic solar cells in terms of power loss density [15] shows that the limited sheet resistance of most transparent conductors, including ITO or their best substitutes, leads to series resistance values that are too high to maintain high power conversion efficiency when the area of the cell is increased. Possible remedies to this limitation include the insertion of connections through via holes to a backside metallic electrode [16], and the so-called stripe geometry in which several cells consisting of narrow stripes are connected in series [17]. However, in the former approach the thin grids and via-hole connections generally suffer from resistances that are still too high and limit the current in large-area cells. The stripe geometry is convenient since it can be used for the manufacturing of large-area modules by roll-to-roll processing. However, it also has its limitations since the area used by the cell-to-cell connections reduces the overall active area of the device, leading to a significant reduction of the power conversion efficiency in modules compared to small-area cells. Like for other photovoltaic technologies, an alternative is to use thick (5–20 μm) metal grid electrodes.

Recently, we reported a detailed study of the area-scaling of organic solar cells based on pentacene / C_{60} and demonstrated improved performance for large-area organic solar cells and modules by integrating metal grids directly with ITO [15,18]. Here, by using electroplated copper grids, the grids can be made fine, reducing the shadowing loss to only 6%, and thicker, resulting in lower resistive losses in large-area devices with higher currents. In fact, the series resistance, which can seriously hinder fill-factor and efficiency, of a large-area OPV device (7 cm^2) with the grid could be kept as small as that of a small-area device (0.13 cm^2) [15].

Another advantage of the thick electroplated grid structure is that it can be processed separately from the organic layers and can be applied to other transparent electrodes.

The aim of this work is to develop a device architecture for large-area OPVs and OLEDs in which ITO is replaced with an inexpensive and crack-tolerant polymer electrode without reducing efficiency. A highly conductive PEDOT:PSS formulation (H.C. Starck, Clevios PH 1000) was selected as a hole-selective electrode and was combined with a thick metal grid structure designed to form good electrical contact with the polymer electrode. This geometry was applied to OPV devices fabricated on glass substrates comprised of pentacene / C₆₀ as the photoactive layers. Although not leading to the most efficient solar cells, pentacene and C₆₀ were selected as model materials for this study because their properties are well characterized [19,20] and because they were selected in our previous detailed study of the area-scaling of organic solar cells [15]. The active area of the devices was 7.3 cm². Performance of cells with the conducting polymer was compared with that of reference pentacene / C₆₀ devices using ITO as the transparent electrode and to devices with a small active area (~0.1 cm²).

2. Experiment

The devices under study were comprised of pentacene as the donor compound, C₆₀ as the acceptor, and bathocuproine (BCP) as an electron transport layer. For the small-area devices, the device geometry was glass / PEDOT:PSS (150 nm) / pentacene (50 nm) / C₆₀ (45 nm) / BCP (8 nm) / Al as shown in Fig. 1. A thin, patterned Au layer (100 nm) was used to optimize the electrical contact between the PEDOT:PSS layer and the Al contact electrode. The PEDOT:PSS (H.C. Starck, Clevios PH 1000) was mixed with 5% by volume of dimethyl sulfoxide (DMSO) to increase its conductivity, spin-coated, and annealed for 20 minutes on a hotplate at 140 °C in air. The organic layers and Al were deposited by thermal evaporation without breaking vacuum between depositions.

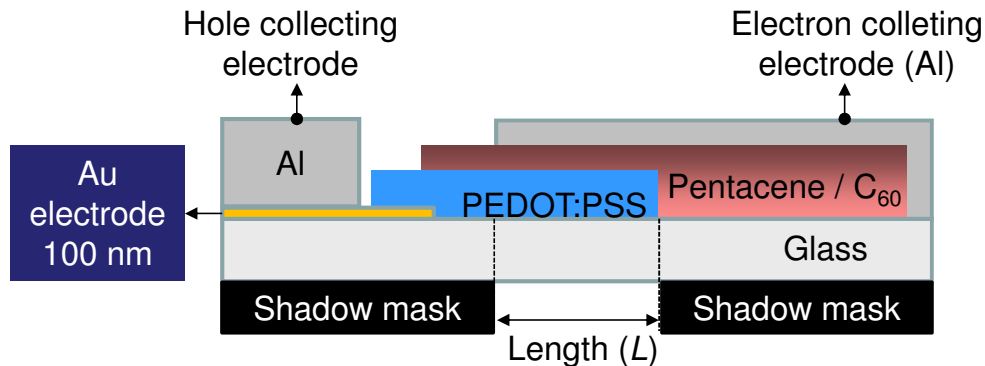


Fig. 1. Device geometry of ITO-free small-area OPV device (0.1 cm²) without a grid.

Substrate preparation: ITO-coated glass was purchased from Colorado Concept Coatings LLC (sheet resistance of 13.7 Ω/sq., 136 nm thick) and diced into 1 inch by 1 inch and 1.5 inch by 1.5 inch squares for the small- and large- area devices, respectively. For the devices with an ITO electrode, the ITO was patterned using chemical wet etching (HCl:H₂O₂:H₂O = 3:1:4) to define the active area. For the ITO-free devices, the ITO was completely removed by using the same chemical etchant.

Metal grid fabrication: For the ITO-free, large-area device, a metal grid was fabricated on top of a glass substrate from which the ITO-coating had been completely removed. 10 nm of chrome and 100 nm of gold were sputtered (Unifilm Technology PVD-300) on the glass and patterned with photolithography to create finger and busbar electrodes. Next, a seed layer of 10 nm of chrome and 150 nm of copper was deposited all over the surface using a filament evaporator (Kurt J. Lesker PVD-75 Filament Evaporator). Electroplating mold structures were created on top of the seed layer with a thick photoresist (Shipley SPR220). Copper

plating solution was prepared by mixing 250 mg of $\text{CuSO}_4 \cdot 5\text{H}_2\text{O}$ and 25 ml of H_2SO_4 in 1 liter of deionized water. 5 μm of copper was electroplated by applying a dc current with a current density of 15 mA/cm^2 . The mold structures were removed using a photoresist remover (Shipley Microposit Remover 1165 at 80 °C for 10 minutes). The electroplated grids were completely passivated with a photoresist (Futurex NR9-8000P) to prevent any electrical shorts between the thick metal grid and the Al top electrode. Finally, the chromium and copper seed layers were removed by wet chemical etching, and part of the Au grid electrode was opened for contact with the to-be-spin-coated polymer electrode. For the large-area device with an ITO electrode, the metal grid only consisted of electroplated copper, which made direct contact with the underlying ITO. The same passivation of the electrodes was used in ITO-free devices and in devices where the electrodes were combined with ITO. The thickness (5 μm) of the metal electrodes was selected based on the power loss density analysis carried out in our previous work [15] where we combined and tested the metal grid with ITO in large-area cells. The thickness achieved here with electroplating is one to two orders of magnitude larger than that of metal grids that were used in conjunction with PEDOT:PSS [12–14] in previous studies aimed at finding a substitute to ITO.

Organic semiconductor processing: For the devices with an ITO electrode, the ITO was cleaned in sequential ultrasonic baths of soap, acetone, and isopropanol for 60 minutes each. Before organic semiconductor deposition, the ITO surface was treated with oxygen plasma and phosphoric acid (20% H_3PO_4 for 10 minutes) [21]. For the ITO-free devices, a polymer electrode was spin-coated from a solution of Clevios PH 1000 PEDOT:PSS (H. C. Starck) mixed with 5% by volume of dimethyl sulfoxide (DMSO) to increase conductivity and annealed for 20 minutes on a hotplate at 140 °C in air. The polymer electrode was patterned to create an active area of 7.3 cm^2 for the large-area device. Then, the devices were transferred into a vacuum thermal evaporator (Spectros, Kurt J. Lesker) connected to a nitrogen-filled glovebox, and pentacene (50 nm, 0.5 Å/s) / C_{60} (45 nm, 1 Å/s) / BCP (8 nm, 0.5 Å/s) / Al (200nm, 1-2 Å/s) were deposited through shadow masks on top of the ITO or PEDOT:PSS electrodes at a base pressure of 2×10^{-7} Torr without breaking vacuum. All of the organic materials were purified at least once by thermal gradient sublimation [22].

Solar cell performance characterization: All photovoltaic properties were measured in a nitrogen-filled glovebox with an AM1.5 G solar simulator (91160, Oriel) as the light source using a Keithley 2400 source meter in a four-wire connection scheme. In this scheme separate pairs of current-carrying and voltage-sensing electrodes are used to make more accurate measurements than with a traditional two-wire scheme. By having low current on the sensing lines to minimize voltage drop, accuracy of the voltage measurement at the device is improved compared to a two-wire scheme.

3. Performance of ITO-free large-area OPV with an integrated metal grid

For the large-area devices, a metal grid was integrated with PEDOT:PSS to reduce the resistive power loss introduced by the PEDOT:PSS electrode. The grid consisted of finger electrodes branching from a busbar to provide low resistance paths for photogenerated holes collected by the PEDOT:PSS electrode. The grids were comprised of patterned thin layers of Au (100 nm) deposited by sputtering and thick electroplated Cu (5 μm) as shown in the cross-sectional view in Fig. 2.

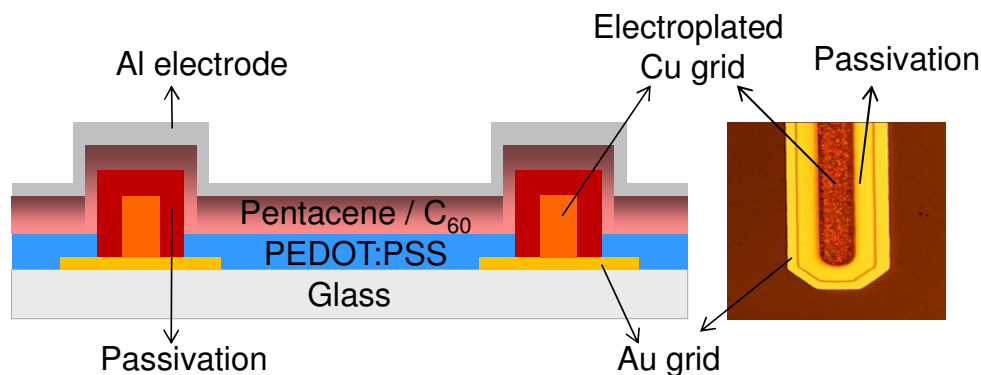


Fig. 2. ITO-free large-area device (7.3 cm^2) with a grid. The grid was composed of two metal layers: sputtered Au (100 nm) and electroplated Cu (5 μm). The thin Au grid connects the PEDOT:PSS electrode to the thick Cu grid. (Media 1)

The thick Cu grid provided very low-resistance current pathways, and its top surface was passivated with photoresist to prevent electrical shorts through the thin organic layers with the top Al electrode. The Cu grid had a finger electrode width of 25 μm , a finger spacing of 2.48 mm, and a busbar width of 300 μm . The patterned Au layer was 80 μm wider than the Cu grid in order to allow for good electrical contact with the PEDOT:PSS layer. Without the Au layer, the passivation of the Cu grid that is carried out to prevent shorts with the top Al electrode makes it difficult to have good electrical contact between the Cu grid and the PEDOT:PSS layer. The entire grid resulted in a 5.5% optical shadowing loss. The PEDOT:PSS layer was spin-coated on top of the grid, followed by the deposition of the photoactive organic layers and the top Al electrode using physical vapor deposition. Measured PEDOT:PSS thickness was 140 nm for the large-area device. The complete device structure is shown in Fig. 3.

Small- and large-area reference devices were also fabricated on ITO (136 nm thick, 13.7 Ω/sq , Colorado Concepts Coatings) glass substrates and their performance compared to that of devices using the conducting polymer as an electrode. For large-area devices with an ITO electrode, electroplated Cu was solely used as a metal grid and caused a 2.2% optical shadowing loss.

When exploring a replacement for ITO, both resistance and optical transmittance of the new electrode must be considered. ITO has a higher transmittance compared with PEDOT:PSS used here for wavelengths greater than 400 nm (Fig. 4). Although the lower transmittance will reduce photocurrent, the small decrease may be a worthwhile trade-off for a lower-cost electrode. To estimate the loss based on the transmission differences alone, the maximum short-circuit current density (J_{SC}) for the AM 1.5 G spectrum transmitted through the transparent electrodes was calculated by integrating the product of the AM 1.5 G spectrum and the transmission spectra from 300 nm to 800 nm, the spectral region where many organic photovoltaic materials absorb. The maximum values of J_{SC} for ITO- and PEDOT:PSS-based devices over this range are 25.4 mA/cm^2 and 23.3 mA/cm^2 , respectively, yielding a total loss of roughly 8% in current. As the open-circuit voltage V_{OC} scales with the logarithm of the short-circuit current [5], its value is not expected to change significantly with an 8% reduction in J_{SC} . Hence, transmission losses are expected to decrease efficiency by less than 10%, which in some cases may be justified by the lower cost and higher flexibility of the polymer electrode. Sheet resistance must also be reasonably low. The sheet resistance of 140 nm-thick layers of PEDOT:PSS was measured using the transmission line method which yielded a value of 98.4 Ω/sq , to be compared with 13.7 Ω/sq for ITO (136 nm).

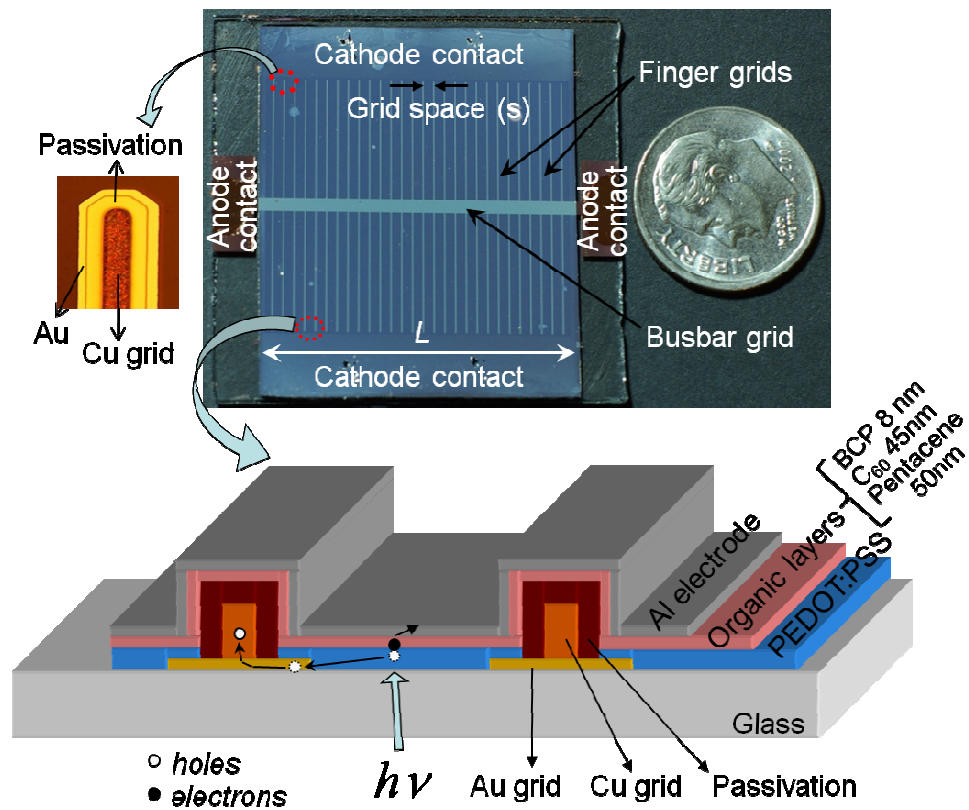


Fig. 3. Complete device. Electroplated thick Cu grid is passivated with photoresist to prevent any electrical shorts with the top Al electrode.

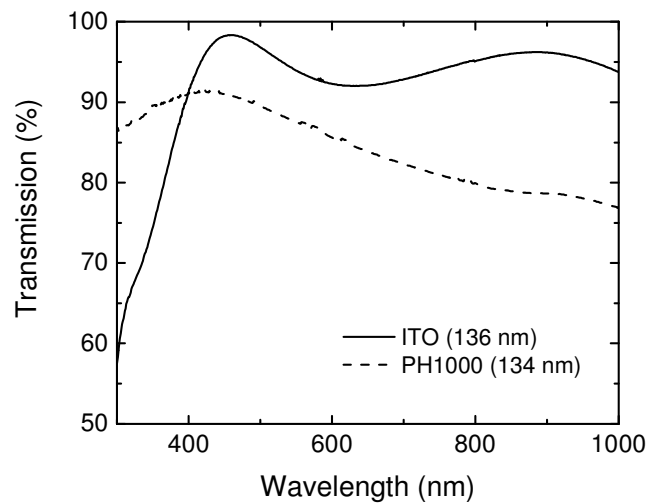


Fig. 4. Optical transmission spectra for 136-nm-thick ITO (solid line) and 134-nm-thick film of PEDOT:PSS (dashed line, Clevios PH1000) on glass substrates.

Figure 5 (a) shows the current-voltage (J - V) curves of small-area devices without a grid in the dark and under illumination with either ITO or PEDOT:PSS as the hole selective electrode, and Table 1 summarizes their performance. Pentacene / C_{60} devices reach an efficiency of 0.8% in devices with a PEDOT:PSS electrode, compared to 1.0% with an ITO electrode, with J_{SC} , open-circuit voltage (V_{OC}), and fill-factor (FF) values all lower compared with those of devices with ITO. The largest drop is in J_{SC} (17%) and cannot be explained by the difference in absorption of the electrode alone. External quantum efficiency (EQE) shown in the inset of Fig. 5 (a) show a larger drop than expected from the transmission data for the PEDOT:PSS device. This difference could possibly be related to a difference in light distribution in the photoactive layers due to interference effects [20] or to a difference in the properties of pentacene due to the different interface it forms with either PEDOT:PSS or ITO. Also, while the series resistance, R_sA , estimated from the inverse of slope in the forward-bias region is higher for PEDOT:PSS compared to ITO, the difference is not significant enough to explain the difference in efficiency.

Figure 5 (b) shows the J - V curves of large-area devices fabricated with either ITO alone, ITO combined with a metal-grid electrode, or PEDOT:PSS with the modified metal-grid electrode. The photovoltaic performance parameters for these three types of devices are summarized in Table 1. The results show that, for large-area devices, a metal grid electrode is essential even when the transparent conductor with the lowest sheet resistance, namely ITO, is used. Without the metal grid, the series resistance R_sA in a device with 7 cm² active area is nearly 22 times higher, decreasing the power conversion efficiency from 0.8% to 0.4%. Note that the photocurrent of both large-area devices with grids is still 20% lower compared to the small-area devices. Optical shadowing effects alone cannot account for this discrepancy which we assign to inhomogeneities in the photoactive films when deposited over large area. As with the small-area devices, J_{SC} was slightly lower for the devices with PEDOT:PSS compared with ITO-based devices, but comparable values for V_{OC} and FF were obtained. The power conversion efficiency for large-area ITO-free devices was 0.7% to be compared with a maximum value of 1.0% measured in small-area ITO-based devices. Also, the series resistance could be reduced for the PEDOT:PSS large-area device relative to the small-area device because the fine grid structure allowed for a smaller average current path length through the PEDOT:PSS to the collecting metal electrode (2.4 mm vs. 4.3 mm). More details about the general effects of grid size on series resistance and performance can be found in Ref [15].

Table 1. Summary of the photovoltaic parameters measured in solar cells with different areas and geometry. Measured R_sA is extracted from the inverse slope of the forward characteristics in Fig. 5. Small cells (0.13 and 0.12 cm²) have one contact while large-area cells (7 and 7.3 cm²) have two contacts on both ends. L is the device length and s is the grid space. Illumination was 96 mW/cm². Average values and standard deviations were based on measurements of 5 devices.

Area [cm ²]		Anode	L or (s) [cm]	J_{SC} [mA/cm ²]	V_{OC} [mV]	FF	η [%]	R_sA (measured) [Ω cm ²]	$R_s^{Calc} A$ [Ω cm ²]
No grid	0.13	ITO	0.46	5.1 \pm 0.5	353 \pm 3	0.55	1.0 \pm 0.1	2.0 \pm 0.6	3.5
	0.12	PEDOT:PSS	0.43	4.2 \pm 0.2	337 \pm 5	0.51	0.8 \pm 0.0	6.8 \pm 1.1	8.6
	7.0	ITO	2.85	4.5	338	0.29	0.4	52	11.8
Grid	7.0	ITO	(0.24)	4.0	341	0.56	0.8	2.4	3.0
	7.3	PEDOT:PSS	(0.24)	3.5	341	0.55	0.7	2.5	3.5

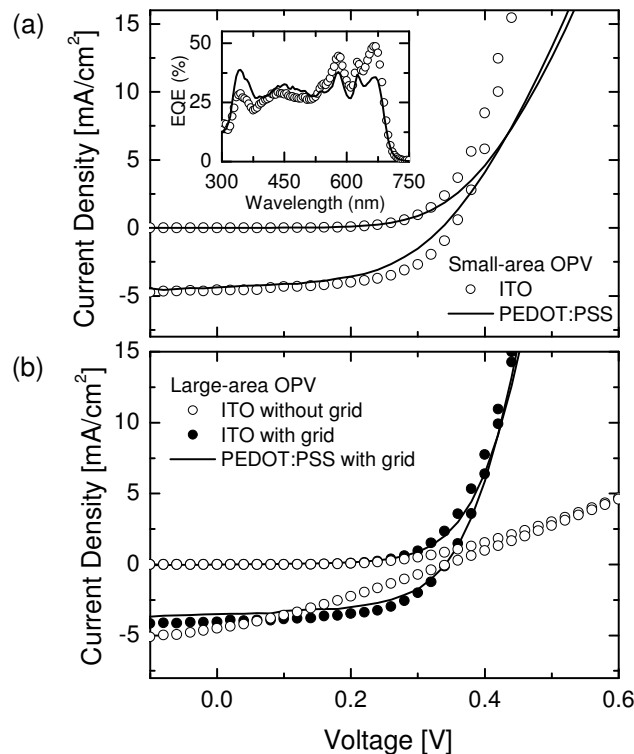


Fig. 5. (a) Experimental J - V characteristics of the small-area devices ($\sim 0.1 \text{ cm}^2$) without a grid and (b) the large-area devices ($\sim 7 \text{ cm}^2$) with and without a grid in the dark and under illumination with either an ITO or PEDOT:PSS hole selective electrode. Inset: EQE for the small-area devices. Solid lines represent devices with a PEDOT:PSS anode while symbols represent devices with an ITO anode.

4. Conclusions

In summary, we demonstrated that an electrode that combines a metal grid and a highly conductive grade of PEDOT:PSS (Clevios PH 1000, H. C. Starck) could be used as a substitute for the conventional ITO-coated substrates. Large-area (7.3 cm^2), ITO-free organic solar cells comprised of pentacene/ C_{60} bilayer heterojunctions yielded power conversion efficiencies of 0.7%. These values have to be compared with 0.8%, the power conversion efficiency measured in devices of similar area with ITO-coated glass electrodes. While PEDOT:PSS exhibits a slightly lower optical transmittance compared with ITO, the overall reduction in photocurrent over the spectral interval [300–800 nm] is estimated to be only 8%. The light shadowing losses introduced by the metal grid are 5.5% which translates into an overall loss of 13% when scaling from small-area ITO-based devices to large-area ITO-free solar cells. Future studies will focus on the fabrication of polymer-based devices on flexible substrates, on their stability, and on their mechanical properties under flexing. The efficiencies obtained in this study with the model devices based on bilayers of pentacene and C_{60} are relatively modest compared to the efficiency of 8.13% achieved recently by Solarmer Energy Inc [23], and certified by NREL. However, power loss density calculations [15] show that the ITO-free device geometry described in this study with electrodes that have a rather high sheet resistance ($98.4 \text{ } \Omega/\text{sq}$) can be easily transposed to record high efficient cells by adjusting the thick metal grid electrode geometry. Organic photovoltaic cells have not yet

reached efficiencies and lifetimes comparable to conventional crystalline silicon cells but continuous advances in material and device geometries bring them a few steps closer to commercialization.

Acknowledgments

The authors thank Prof. Ajeet Rohatgi and his research group at Georgia Institute of Technology for fruitful discussions. This material is based upon work supported in part by the STC Program of the National Science Foundation under Agreement No. DMR-0120967 and by the Office of Naval Research. This work was performed in part at the Microelectronics Research Center at Georgia Institute of Technology, a member of the National Nanotechnology Infrastructure Network, which is supported by NSF (Grant No. ECS- 03-35765).